J. Fluid Mech. (2015), vol. 785, R3, doi:10.1017/jfm.2015.668



JFM RAPIDS
journals.cambridge.org/rapids

Oscillations in cylinder wakes at Mach 4

B. E. Schmidt[1],† **and J. E. Shepherd**[1]

[1]Department of Aerospace Engineering, California Institute of Technology, Pasadena, CA 91101, USA

(Received 3 August 2015; revised 13 October 2015; accepted 8 November 2015; first published online 23 November 2015)

The wake behind a circular cylinder in Mach 4 flow is examined experimentally in the Reynolds number range 2×10^4 to 5×10^5. Periodic oscillations of the sliplines in the wake are observed. The Strouhal number of the oscillations based on the diameter of the cylinder is found to increase monotonically from 0.30 to 0.50 with increasing Reynolds number. If the Strouhal number is formed using the length of the sliplines, however, it has a constant value of approximately 0.48 for all Reynolds numbers studied. This scaling indicates that the oscillations in supersonic flow are likely driven by acoustic signals propagating back and forth through the subsonic region between the separation points on the cylinder and the neck where the sliplines converge, unlike in subsonic flow where oscillations are caused by vortices shed from the cylinder surface.

Key words: aerodynamics, high-speed flow, wakes

1. Introduction

The phenomenon of vortex shedding in the wakes behind bluff bodies in incompressible flow has been widely studied across a broad range of Reynolds numbers over the last century. Some of the more notable early work was performed by Roshko. He records drag coefficients and Strouhal numbers for the periodic vortex shedding for Reynolds numbers in the range 40–10 000 (Roshko 1953) and above 10^6 (Roshko 1961). Roshko also developed a famous result, namely that a universal Strouhal number exists for Reynolds numbers in the irregular range ($Re > 300$) using the wake width d_w and a characteristic wake velocity U_s to scale the frequency of vortex shedding (Roshko 1954):

$$St^* = \frac{f d_w}{U_s}. \tag{1.1}$$

The value for St^* is found to be approximately 0.164 across a wide range of Reynolds numbers and bluff body shapes besides cylinders. For a more complete, though

† Email address for correspondence: bryan.e.schmidt@gmail.com

© Cambridge University Press 2015

https://doi.org/10.1017/jfm.2015.668 Published online by Cambridge University Press

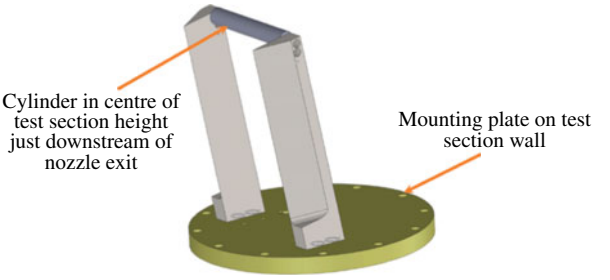


FIGURE 1. Perspective view of the 19.05 mm diameter cylinder in the mount. Flow is from left to right in the figure, orthogonal to the cylinder.

certainly not exhaustive, review of work on bluff body wakes in incompressible flow see Williamson (1996).

Compared to work in subsonic flow, studies of supersonic flow past circular cylinders are relatively sparse. Gowen & Perkins (1953) detailed the flow structure behind a cylinder in supersonic flow and performed experiments over a Mach number range of 0.3–2.9 and Reynolds number ranges of 50 000–160 000 and 100 000–1000 000 to measure drag coefficients. Figure 4 of that report shows a shadowgraph image detailing the primary flow features. Kim (1956) performed a similar study across a range of Mach numbers from 1.35 to 6.0. More recently numerical studies were performed by Bashkin *et al.* (1998, 2000, 2002) with emphasis on the pressure and temperature distributions on the cylinder surface and the location of the separation point at various Mach and Reynolds numbers. To the authors' knowledge no experimental work has been performed to determine if there are oscillating flow features in the wake behind cylinders in supersonic flow as there are in subsonic flow. The goal of the present study is to make such a determination by carefully studying the flow behind cylinders at Mach 4 at various Reynolds numbers in the range 2×10^4 to 5×10^5.

2. Experimental methods

Experiments were carried out in the Mach 4 Ludwieg tube at Caltech. The Caltech Ludwieg Tube is a free-jet wind tunnel that produces Mach 4 flow from a 300 mm-diameter nozzle exit. The free-stream velocity is 670 m s^{-1} and the stagnation pressure can be varied between 100 and 600 kPa, corresponding to a unit Reynolds number ($\rho_\infty u_\infty/\mu_\infty$) range of 5×10^6 to 25×10^6 m^{-1}. The tunnel operates with a pneumatic fast-acting valve in the nozzle throat similar to the one described in Estorf, Wolf & Radespiel (2003) and has a run time of approximately 60 ms.

A set of four precision-ground aluminium cylinders were used in the experiments. All four are 127 mm long but have diameters of 3.2, 7.9, 19.0, and 44.5 mm. Each cylinder was tested at unit Reynolds numbers of 6.6×10^6 and 11×10^6 m^{-1}. The mount, shown in figure 1, was designed to minimize end effects by diverting the supersonic free stream away from the centre of the cylinder while still allowing the wake of the cylinder to be fully visible. Shadowgraph images are acquired with a Phantom v710 CMOS camera. Low-speed images of the full flow field are taken using a continuous white light Cree X-Lamp LED for illumination. High-speed data is taken using a pulsed 670 nm laser diode with a frame rate of 200 000 f.p.s. and a pulse width of 20 ns. This technique is described in detail by Parziale *et al.* (2015).

https://doi.org/10.1017/jfm.2015.668 Published online by Cambridge University Press

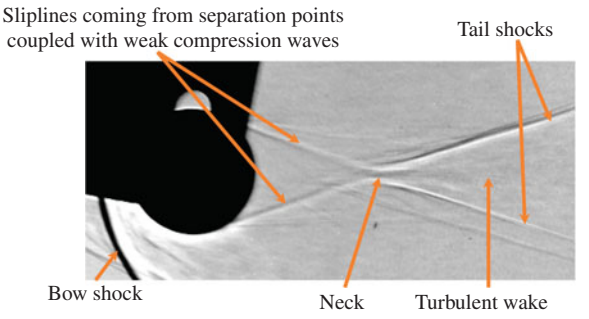


FIGURE 2. Shadowgraph image of the 19.05 mm diameter cylinder at a Reynolds number of 2.1×10^5 taken with the white light LED source to show the mean flow structure.

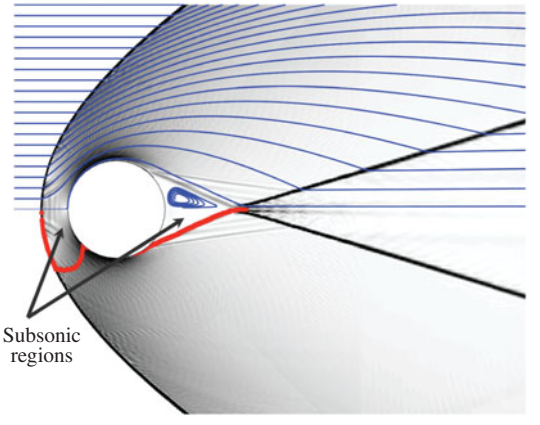


FIGURE 3. Sketch of flow field around the cylinder. The top of the image shows streamlines (blue) and the bottom of the image shows the location of the sonic lines (red). Note that there is a subsonic region immediately behind the cylinder bounded by the cylinder surface and the sliplines.

3. Results

A single shadowgraph image taken with the white light LED source is shown in figure 2 to show the mean flow structure. The cylinder shown is the 19.05 mm-diameter cylinder at a Reynolds number based on diameter of 2.1×10^5 and the flow features are similar for all cases studied. Behind the cylinder, sliplines extend from the separation points on the cylinder and converge to a finite width at the 'neck' of the wake. Tail shocks are generated at the neck that turn the flow so that it is again parallel after converging behind the cylinder.

An Euler computation with AMRITA (Quirk 1998) was performed to lend additional insight into the flow structure behind the cylinder. A movie of the result is available at http://dx.doi.org/10.1017/jfm.2015.668. The computation reveals that the region bounded by the sliplines, the cylinder surface and the neck is subsonic and contains a counter-rotating vortex pair. Sonic lines lie just inside the sliplines. This finding is corroborated by the computations of Bashkin *et al.* (2000, 2002). A sketch of the flow field with these features is shown in figure 3. Unlike in subsonic flow, flow

https://doi.org/10.1017/jfm.2015.668 Published online by Cambridge University Press

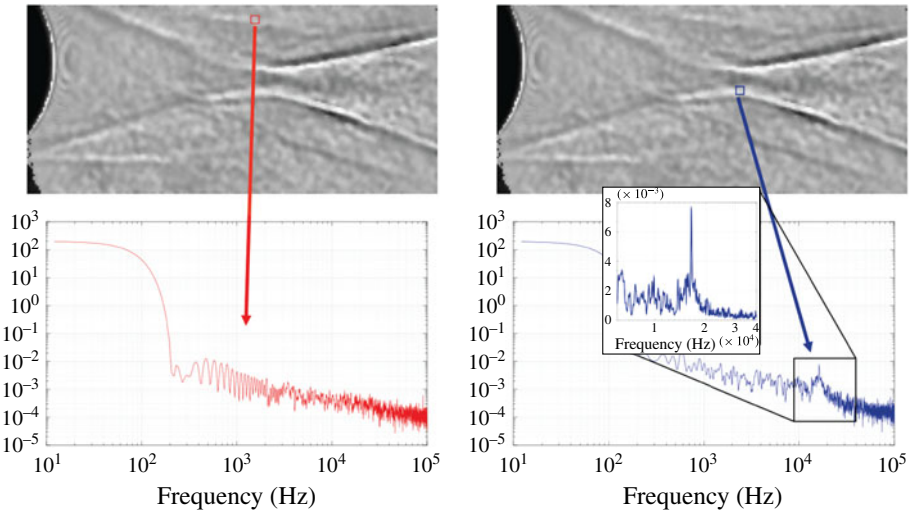


FIGURE 4. Shadowgraph images taken with the pulsed laser light source with boxes marking sampling locations with corresponding spectra. The sampling location on the right produces a peak in the spectrum at approximately 16 kHz.

separation on the cylinder does not occur due to an adverse pressure gradient on the rear of the cylinder. Indeed, in supersonic flow the pressure gradient is favourable on the cylinder surface due to the expansion fan in the flow over the cylinder. Separation in this flow occurs instead because of a limitation on flow turning angle through the tail shocks after the flow has been turned by the expansion fan. Bashkin *et al.* (1998) showed that the separation point location does vary weakly with both the Mach and Reynolds numbers in supersonic flow: between 114° and 125°, measured from the front stagnation point, in Mach 2 flow and between 117° and 130° in Mach 5 flow for Reynolds numbers from 10^4 to 10^8. Our experiments show separation angles between 105° and 120° for the Reynolds numbers studied. This variation indicates that flow separation is not entirely an inviscid phenomenon in this flow.

Our Euler computations predict that the sliplines oscillate at the neck. This prediction was investigated using the pulsed laser diode light source to take high-speed, short-exposure shadowgraph images. A series of approximately 10 000 images was acquired at 200 000 f.p.s. for each cylinder at each unit Reynolds number. An example movie available at http://dx.doi.org/10.1017/jfm.2015.668. The intensity of a small portion of each image is sampled at a fixed location in space near the neck and a Fourier analysis is performed in time to detect oscillations. Figure 4 illustrates the method and shows a sample power spectrum. The shadowgraph images are for the same conditions as those shown in figure 2. On the left, the image is sampled over the red square far from the neck and the resulting power spectrum is shown below with no discernible peaks. On the right, the image is sampled over the blue square in the region of the neck and a peak is detected at approximately 16 kHz for this cylinder and Reynolds number. This result is repeatable for sampling locations near the neck, and the magnitude of the peak in the power spectral density is a factor of 8–10 above the average baseline signal.

https://doi.org/10.1017/jfm.2015.668 Published online by Cambridge University Press

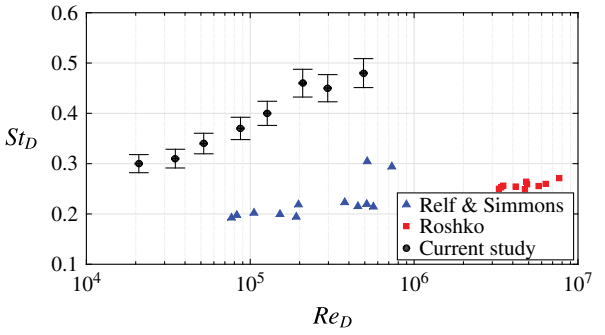


FIGURE 5. Strouhal number versus Reynolds number for cylinder wake oscillations.

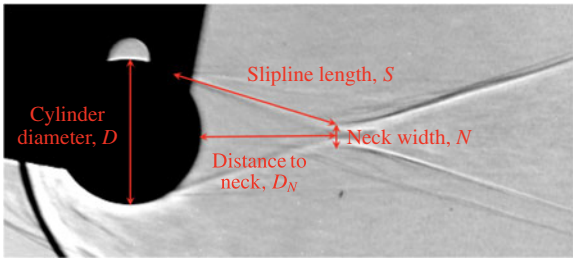


FIGURE 6. Relevant length scales in the flow field.

4. Discussion

Oscillation frequency is plotted as Strouhal number based on diameter,

$$St_D = \frac{fD}{U_\infty}, \tag{4.1}$$

versus Reynolds number based on diameter,

$$Re_D = \frac{U_\infty D}{\nu_\infty}, \tag{4.2}$$

in figure 5. Data from Relf & Simmons (1924) and Roshko (1961) for incompressible flow are shown for comparison. The uncertainty in St_D is based on estimates of the full-width at half-maximum of the frequency peak in the power spectral density. The Strouhal number is observed to increase with increasing Reynolds number with a power-law dependence as it does in incompressible flow. The Strouhal number in supersonic flow is found to be substantially higher than that in subsonic flow at the same Reynolds number, but a disagreement is not unexpected as the mechanisms for the oscillations in the two flow regimes are likely different.

We now examine the notion of a universal Strouhal number using a length scale other than the diameter. The velocities in the inviscid regions of the flow are assumed to not depend on Reynolds number so the free-stream velocity will still be used to form the universal Strouhal number. This approximation is shown to work well in incompressible flows at high Reynolds number as well by Fage & Johansen (1927). Figure 6 is similar to figure 2 but instead shows the relevant length scales in the flow: cylinder diameter D, slipline length S, distance to the neck D_N, and neck width N.

https://doi.org/10.1017/jfm.2015.668 Published online by Cambridge University Press

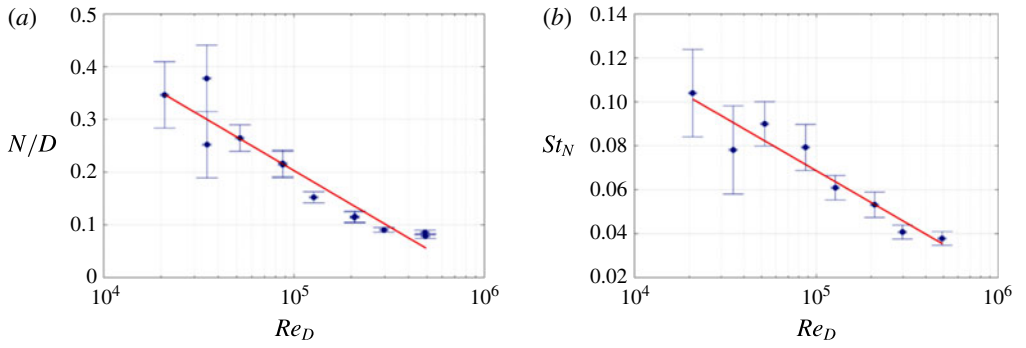


FIGURE 7. (*a*) Variation of neck width with Reynolds number, (*b*) variation of Strouhal number based on neck width versus Reynolds number.

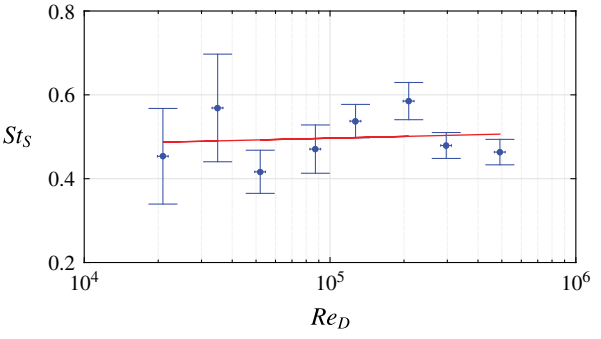


FIGURE 8. Strouhal number based on slipline length versus Reynolds number.

The neck width N is analogous to the width of the wake d_w used in the definition of the universal Strouhal number by Roshko in (1.1). Figure 7 shows the variation of the non-dimensional neck width N/D with Reynolds number and the Strouhal number based on the neck width versus Reynolds number. The scaled neck width decreases with increasing Reynolds number, but scaling the frequency of oscillations by the neck width does not form a universal Strouhal number that is constant across the Reynolds number range. This suggests that the mechanism for oscillation is different in supersonic and subsonic flow.

A physically motivated choice of length scale can be made by more closely considering the mechanism of the oscillations. In our Euler computations the oscillations appear to result via communication between the separation points on the cylinder and the ends of the sliplines at the neck. Acoustic signals cannot propagate upstream from the neck to the separation points in the supersonic region outside the sliplines, but since the flow is subsonic inside the sliplines, information can travel both upstream and downstream along trajectories just inside the sliplines. This mechanism suggests that the relevant length scale by which to scale the oscillation frequency should be the slipline length S. Figure 8 shows the Strouhal number based on slipline length

$$St_S = \frac{fS}{U_\infty} \tag{4.3}$$

https://doi.org/10.1017/jfm.2015.668 Published online by Cambridge University Press

plotted versus Reynolds number. It does not have a systematic dependence on Reynolds number and has a value of approximately 0.48 for $10^4 < Re < 10^6$. This supports our hypothesis that the oscillations are sustained by communication between the neck and separation points along the sliplines. If they were not, we would not expect the slipline length to produce a universal Strouhal number as is shown in figure 8.

The driving force behind the oscillations is unclear. Our Euler computations predict that the separation point locations move back and forth very slightly, which would suggest that perhaps unsteadiness in the separation point location drives the oscillation and the motion of the sliplines at the neck supplies sustaining feedback. Motion of the separation points was not detected in our experiments, which indicates that either the amplitude of their motion is too small to be detected by our optical system or that another mechanism is at work. A possible alternative mechanism is that the oscillations in the sliplines are driven by other flow features inside the neck, and the separation region acts as an acoustic resonator. Of course we cannot rule out the possibility that the oscillations we observe are due to other global or convective instabilities, such as a longitudinal Kelvin–Helmholtz instability such as that observed in the numerical studies of Sandberg & Fasel (2006) and Sandberg (2012), but the scaling of the universal Strouhal number is consistent with acoustic resonance. It is also possible that a global or convective instability provides an initial perturbation that triggers acoustic resonance in the subsonic region, resulting in the observed oscillation.

5. Conclusions

In this study we have shown for the first time that periodic oscillations occur in the wake behind a cylinder in supersonic flow at Mach 4. If the frequency of these oscillations is non-dimensionalized into a Strouhal number based on the diameter of the cylinder, the Strouhal number is found to increase with the free-stream Reynolds number for the conditions studied as it does in subsonic flow at the same Reynolds numbers. Furthermore, if the Strouhal number is formed using the length of the sliplines from the separation points to the neck behind the cylinder instead of the cylinder diameter, this Strouhal number is universal for the Reynolds numbers studied. This scaling indicates that the mechanism sustaining the oscillations is the propagation of acoustic waves between the separation points and the neck through the subsonic region inside the sliplines. As this is the first study of its kind, it would be interesting to study this phenomenon at other Reynolds numbers and Mach numbers to further validate the universal scaling presented here and also to perform studies with other measurement techniques to lend additional insight into the mechanism driving the oscillations. Detailed, viscous numerical simulations and stability calculations would also be very useful in understanding the observed phenomena.

Acknowledgements

The authors would like to thank Professor H. Hornung for performing the Euler computations used in this work. Additional thanks are due to A. Kiani and J. Haggerty for their work machining the models and mount. Finally, the authors would like to thank B. Valiferdowsi for assistance in the laboratory. B.E.S. acknowledges the support of the Foster and Coco Stanback STEM Fellowship for his graduate studies.

https://doi.org/10.1017/jfm.2015.668 Published online by Cambridge University Press

Supplementary movies

Supplementary movies are available at http://dx.doi.org/10.1017/jfm.2015.668.

References

BASHKIN, V. A., EGOROV, I. V., EGOROVA, M. V. & IVANOV, D. V. 1998 Initiation and development of separated flow behind a circular cylinder in a supersonic stream. *Fluid Dyn.* **33** (6), 833–841.

BASHKIN, V. A., EGOROV, I. V., EGOROVA, M. V. & IVANOV, D. V. 2000 Supersonic laminar-turbulent gas flow past a circular cylinder. *Fluid Dyn.* **35** (5), 652–662.

BASHKIN, V. A., VAGANOV, A. V., EGOROV, I. V., IVANOV, D. V. & IGNATOVA, G. A. 2002 Comparison of calculated and experimental data on supersonic flow past a circular cylinder. *Fluid Dyn.* **37** (3), 473–483.

ESTORF, M., WOLF, T. & RADESPIEL, R. 2003 Experimental and numerical investigations on the operation of the Hypersonic Ludwieg tube Braunschweig. *Tech. Rep.* Technical University at Braunschweig.

FAGE, A. & JOHANSEN, F. C. 1927 On the flow of air behind an inclined flat plate of infinite span. *Proc. R. Soc. Lond.* A **116** (773), 170–197.

GOWEN, F. E. & PERKINS, E. W. 1953 Drag of circular cylinders for a wide range of Reynolds numbers and Mach numbers. *Tech. Rep.* Technical Note 2960. National Advisory Committee for Aeronautics.

KIM, C.-S. 1956 Experimental studies of supersonic flow past a circular cylinder. *J. Phys. Soc. Japan* **11** (4), 439–445.

PARZIALE, N. J., DAMAZO, J. S., SCHMIDT, B. E., WANG, P. S., HORNUNG, H. G. & SHEPHERD, J. E. 2015 Pulsed laser diode for use as a light source for short-exposure, high-frame-rate flow visualization. In *AIAA SciTech 2015*, AIAA.

QUIRK, J. J. 1998 AMRITA: a computational facility (for CFD modelling). *Lecture Series – von Karman Institute for Fluid Dyn.* **3**, D1–D72.

RELF, E. F. & SIMMONS, L. F. G. 1924 The frequency of eddies generated by the motion of circular cylinders through a fluid. *Aero. Res. Couc., Lond.*, Rep. and Mem. no. 917.

ROSHKO, A. 1953 On the development of turbulent wakes from vortex streets. NACA *Tech. Rep.* TN 2913. National Advisory Committee for Aeronautics.

ROSHKO, A. 1954 On the drag and shedding frequency of two-dimensional bluff bodies. *Tech. Rep.* 3169. National Advisory Committee for Aeronautics.

ROSHKO, A. 1961 Experiments on the flow past a circular cylinder at very high Reynolds number. *J. Fluid Mech.* **10** (3), 345–356.

SANDBERG, R. D. 2012 Numerical investigation of turbulent supersonic axisymmetric wakes. *J. Fluid Mech.* **702**, 488–520.

SANDBERG, R. D. & FASEL, H. F. 2006 Numerical investigation of transitional supersonic axisymmetric wakes. *J. Fluid Mech.* **563**, 1–41.

WILLIAMSON, C. H. K. 1996 Vortex dynamics in the cylinder wake. *Annu. Rev. Fluid Mech.* **28**, 477–539.

https://doi.org/10.1017/jfm.2015.668 Published online by Cambridge University Press